Effect of alkyl chains configurations of tertiary amines on uranium extraction and phase stability – part II: Curvature free energy controlling the ion transfer

Zijun Lu, Sandrine Dourdain, Jean-François Dufrêche, Bruno Demé, Thomas Zemb, S Pellet-Rostaing

Version of Record: https://www.sciencedirect.com/science/article/pii/S0167732222000228
Manuscript_43184d5f0232cfd41b311dcc35089f02

Effect of alkyl chains configurations of tertiary amines on uranium extraction and phase stability - Part II: curvature free energy controlling the ion transfer

Zijun Lu[1], Sandrine Dourdain[1], Jean-François Dufrêche,[1] Bruno Demé,[2] Thomas Zemb[1] and Stéphane Pellet-Rostaing[1]
[1] ICSM, Univ Montpellier, CEA, CNRS, ENSCM, Marcoule, France
[2] Inst. Laue Langevin, Grenoble, France

Abstract

We consider a structural and thermodynamic analysis of uranium solvent extraction by tertiary amines for which the alkyl chain configuration has been modified. The first part of this work revealed that tertiary amines with longer or branched alkyl chains allow tuning the phase stability and uranium extraction by modifying the volume of the polar species extracted in the organic phase. A complete fit of SANS data confirms in this second part that this phenomenon is related to the supramolecular self-assembly of the tertiary amines into smaller reverse micelle like aggregates for longer or branched alkyl chains. It moreover shows that these smaller aggregates quench third phase formation thanks to reduced attractive interactions between them. A thermodynamic analysis based on the "ienaic" approach further rationalizes this effect by showing that alkyl chains have a significant effect on the aggregate's curvature free energy. The latter becomes a predominant inhibitor of uranium free energy of transfer due to the high entropic contribution originated by the extractants branching and packing.

Introduction

Solvent extraction is the method of choice applied in many industrial processes dedicated to metal recovery.[1] First studied empirically for historical applications, the knowledge of the mechanisms underlying solvent extraction processes are nowadays considered mandatory for their optimization.[2]

Traditionally, the so-called "slope method" is applied to determine an apparent stoichiometry of the metallic species extracted in the organic solvent. Based on the mass action law, i.e., ignoring any volume effect in the polar cores-, the "slope method" used in chemical engineering leads to determination of the coordination number determination by the log-log plots of the extracted metal distribution coefficient vs the log of extractant concentration. The coordination number is defined as the number of extractants directly coordinated to each

extracted cation, and is distinct from the aggregation number, that is the number of molecules par aggregate.[3] However, it has been noticed on several examples that the complex extraction mechanisms cannot be summarized with equilibria with well-defined stoichiometry.[4–6] For instance, deriving such complex stoichiometry from the variation of a distribution coefficient cannot account for the real structure of the organic phase.

Indeed, in addition to the strict extractant complexes necessary to chelate the cation to extract, it has been shown that the organic phase is composed of large amount of extractants in monomeric form, and weakly bounded extractant forming supramolecular aggregates that are comparable to reverse micelles.[3] The pseudo-phase approach introduced by Charles Tanford [7] applies here: monomers of extractant that are in the "bulk" pseudo-phase" are in dynamic equilibrium with aggregated extractants. Using the misleading "slope method" cannot account for all these effects.

As already mentioned in Part I, mechanisms underlying various features as acid and diluent effect,[8–10] third phase formation[11–13] or synergistic mixtures of extractants[14,15] could be rationalized by taking into account complexation associated to extractant aggregation effects. It is not simple to disentangle chelation and aggregation mechanisms as they are usually coupled.[16,17] Experimentally, one strategy is to modify parameters as extractant or diluent alkyl chains and measure all distribution coefficients to clearly isolate effect of aggregation from the extraction free energy. Studying lanthanide extraction by diglycolamides, Stamberga *et al.*[18] demonstrated with such a structure-performance relationship approach, that subtle steric changes markedly affect extraction and selectivity trends in lanthanides separation through electrostatic interactions occurring beyond the first coordination sphere of the metals extracted. This strategy was also followed in our study with tertiary amines extractants for uranium extraction, showing that alkyl chain length and branching significantly modify the extraction of polar species and the organic phase stability. This pure aggregation effect needs to be rationalized.

With a thermodynamic analysis Zemb et al., showed that considering the "motor" of complexation only is much too strong to explain the typical values of distribution coefficient obtained in solvent extraction.[3,19,20] In the colloidal approach called "ienaics",[21] it was shown that a more general view going beyond molecular complexation considerations is necessary to account for the ion transfer from aqueous phase to organic phase. The Gibbs energy of ion transfer is decomposed in four terms, which take into account complexation as well as long range interactions in order to give insights on the origin of ion transfer.

The complexation with the first neighbors is a strong term of typically 50 kJ/mol per extracted species that allows the transfer to the oil phase.[20] This term is counter balanced by three weaker quenching terms:

- The “bulk” term or “droplet” term, corresponds to the free energy of a droplet of confined aqueous electrolyte solution in the core of the aggregates. This term models the entropic cost to pack the hydrophilic electrolytes inside the polar core of the aggregates. It can be calculated by considering the measured concentrations of water, acid and metals extracted in the organic phases.
- The “chain” term, is the sum of the curvature energy and of the micellisation energy of the aggregates:
    - curvature energy represents the free energy of the extractants arrangement in the aggregates. It is associated with the variation of the shape and size of the reverse micelles which can be calculated from X-ray or neutrons scattering (aggregate and core radii), or from molecular mesoscopic simulations to provide the bending constant κ^* and the spontaneous and effective packing parameters.[17]
    - micellisation free energy of the aggregates, can be calculated with the critical aggregation concentration (CAC) that can be derived from SAXS and SANS fitting or from surface tension measurements.

Based on these assumptions, Špadina *et al.* developed a theoretical model which allows quantitative estimation of free energies of ion transfer.[17,22,23] Successful application of “ienaic” approach have also been reported for neutral solvating extractant system,[22] for acidic extractant system,[17] as well as for synergistic extractants system.[24]

We propose here to apply such a thermodynamic analysis on the tertiary amines used in the AMEX process for uranium production in the front-end nuclear fuel cycle. As in the first part of this work, extraction of two principal types of tertiary amines are considered to provide a complete description of the effect of alkyl chain length and branching on aggregation and extraction:

- a first group of 5 molecules with linear alkyl chains but different chains length: Trihexylamine (C6 THA), Tri-heptylamine (C7 THA), Tri-octylamine (C8 TOA), Tri-nonylamine (C9 TNA) and Tri-decylamine (C10 TDA);
- a second group of 3 molecules with the same carbon number on the alkyl chains but different branching situation: Tri-octylamine (C8 TOA), Tri-isooctylamine (C8 TIOA) and Tris(2-ethylhexyl)amine (C8 TEHA).

The two series of amines are presented in Figure 1.

(a)

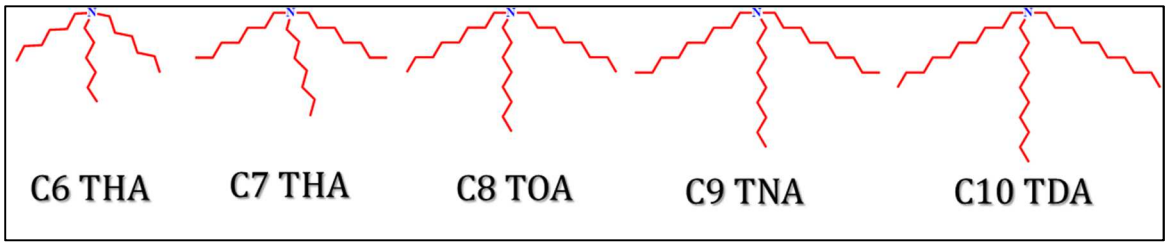

(b)

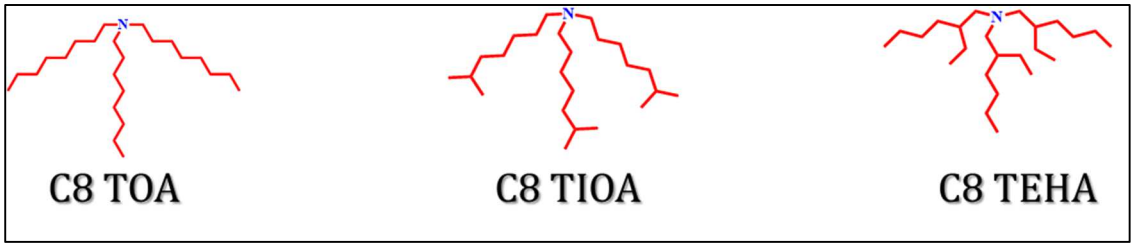

Figure 1. Molecular structures of tertiary amines (a) with different carbon number on the linear alkyl chains and (b) with 8 carbons but different branched groups on the alkyl chains.

We showed in the first part of this study that tertiary amines with longer or more branched alkyl chains allow improving the phase stability and decrease uranium extraction when cumbersome branching are applied. These effects appeared to be related to smaller volume of the polar species extracted in the organic phase, as well as aggregates. To provide a deeper understanding on the alkyl chains configuration effect on extraction and aggregation and to decorrelate the thermodynamic motors responsible for such properties, we apply in this second part a complete thermodynamic analysis based on the "ienaic" approach and on the modeling of the scattering data.

Methods

In this article, the experimental results collected in Part I are analyzed with a SANS modelling to interpret quantitatively the aggregation properties of the various tertiary amines tested, and further interpreted with a thermodynamic model. Details of the applied models are described in the following.

SANS modelling

SANS data were fitted with a model considering a form factor of spherical particles with a core-shell form factor and a Baxter's sticky hard sphere structure factor.[12,25] In this model, a polar core containing the extracted solutes and the polar heads of the tertiary amines, is distinguished from the apolar shell composed of the alkyl chains of the tertiary amines and the penetrated octanol molecules. Concentrations of extracted solutes were used to estimate

the scattering length densities of the core of the aggregates and the volume fraction of the scattered objects. As they are constant in this Q range, contributions of the solvent and of the incoherent have been added as a constant term in the calculated spectra.

We use in this work the model of sticky hard monodisperse sphere of Baxter in order to calculate scattering and to estimate order of magnitude of effective hard sphere and effective short range interaction potential.

It must be noticed that there are three different difficulties inherent to the Baxter model:

a-the reverse aggregates are not *hard* spheres, since they are produced by dynamical exchange: there is no contact and bouncing, but fast exchange of molecules. Introducing hard steric walls introduces artefacts.

b- the water in oil aggregates is very polydisperse. This polydispersity makes those oscillations of the form factor not apparent, and uncontrolled errors are induced in adjustments.

c- the stickiness is an effective value, with range less than 10% of the core radius. This is not the case since two attractive phenomena come in: dispersion forces as well as coalescence of droplets becoming infinite connected networks.[26] The numerical values of the stickiness parameter is not representative of an interaction only, but of a shape morphology.

Despite these problems, the Baxter model remains a simple procedure to fit scattering in terms of P(q) and S(q), and we used it in this work. The two other analytical models: Debye-Anderson-Brumberger,[27] in the absence of steric repulsion and the fluctuation Ornstein-Zernike models.[28] In the absence of analytical model, the only remaining method is to calculate the expected SAXS directly from the MD snapshots using any of the standard routines available in libraries. However, boxes large enough to contain a representative coalescing curved interfacial layers are difficult to make.

A polydispersity was introduced on the polar core size and on the shell thickness to obtain an optimal fit. The polydispersity ratio, *PD*, defined by the ratio between the standard deviation and the radius/thickness was fitted for each sample. Signal of the pure deuterated solvent was measured and considered constant to be added according to its volume fraction in each sample.

The principal parameters determined from the fit are the polar core radius r_{core} ; the aggregates shell thickness Δt_{shell}; and the stickiness parameter τ^{-1}, which value characterizes the strength of the sticky hard sphere attractive forces at short distances. Considering that polar cores contain all the extracted solutes and the polar parts of the extractant molecules and by estimating the average volume of extracted solutes per extractant, the average number

of extractant molecules per aggregate N_{agg} was derived from the obtained r_{core}. Equations used for the fit are detailed in Supporting Information.

The parameters including N_{agg}, r_{core} and Δt_{shell} are crucial to determine the thermodynamic motors responsible for the uranium transfer.

Thermodynamic motors responsible for the uranium transfer

The "ienaic" approach.[3] estimates the main driving forces responsible for the transfer of metallic ions from aqueous phase to organic phase, by taking into account the aggregation of extractant molecules. A thermodynamic balance expresses the total free energy of transfer $\Delta G_{transfer}$ as a function of several "driving forces" that control the partition of electrolytes between the organic and the aqueous phase.[19,20]

In this work, we consider that the free energy of transfer of one cation is the combination of three driving forces taking into account entropic and enthalpic effects of complexation and of supramolecular aggregation of extractants:

$$\Delta G_{transfer} = \Delta G_{complexation} + \Delta G_{droplet} + \Delta G_{chain}$$

Where

$$\Delta G_{chain} = \Delta G_{micellisation} + \Delta G_{curvature}$$

Equation 1

Among these three terms, complexation between the extracted ions and the extractant is a strong term of approximately 30-50 k_BT per extracted species that favors the transfer to the oil phase.[20] This term is counterbalanced by weaker quenching terms due to the formation of aggregates in the organic solution, the packing of extractants chains, and the packing of the solutes confined in the polar part of the aggregates.

- *Transfer energy*

The uranium apparent Gibbs free energy of transfer, denoted $\Delta G_{transfer}(UO_2^{2+})$ is defined as follows:

$$\Delta G_{transfer}(UO_2^{2+}) = -k_BT.\ln D_U$$

Equation 2

With k_BT the thermal energy, D_U the distribution ratio of uranium, and considering **one** UO_2^{2+} per aggregate.

- *Complexation term*

The value of $\Delta G_{complexation/agg}$ is here expressed per aggregate and per extracted uranyl ion.

The complexation energy of extractant molecules toward actinides in apolar diluents is difficult to determine using classical approaches because it is commonly determined in polar

diluents (for example with UV/vis measurements). In this work, an estimation is proposed by considering the values of literature.

- *Droplet term*

The second term denoted "droplet term" is due to aggregation. It is related to the confinement of ions in the very small polar volumes in the oil phase. It is the entropic energy associated with the packing of hydrophilic species inside the polar core of the aggregates. In this work, the hydrophilic species include the extracted metallic ions, co-extracted water and salts, and the extractant polar heads.

As the concentration of extracted uranyl in the organic phase is low compared to the concentration of ligand, all the aggregates formed in the organic phase do not contain uranyl. Therefore, two types of aggregates with and without uranyl (noted $agg_{with\ UO_2^{2+}}$ and $agg_{no\ UO_2^{2+}}$ respectively) can be distinguished. Only the aggregation terms of the aggregates containing uranyl cations were therefore considered for the thermodynamic calculation of the transfer of these uranyl cations.

Considering that all the extracted acid molecules participate to the protonation of amines molecules, the droplet term relies on the following chemical equilibrium:

$$(UO_2^{2+})_{aq} + \boldsymbol{i}(H_2SO_4)_{aq} + \boldsymbol{j}(H_2O)_{aq} + \boldsymbol{N_{agg}}(R_3N)_{org} \leftrightarrow (\boldsymbol{N_{agg}} - \boldsymbol{2i})(R_3N)_{org} + \boldsymbol{i}(R_3NH^+)_2(SO_4^{2-})_{org} + (UO_2^{2+})_{org} + \boldsymbol{j}((H_2O)_{org}$$

Equation 3

Where $\boldsymbol{i}$ and $\boldsymbol{j}$ stand for the stoichiometric coefficient of H_2SO_4 and H_2O in the aggregates containing **1** uranyl.

According to the equations proposed by Dufreche and Zemb [20] and Rey *et al.*,[24] the droplet term can be expressed as follows:

$$\Delta G_{droplet}(UO_2^{2+}) = \boldsymbol{i}\ln\left(\frac{m_{SO_4^{2-}}^{org}\gamma_{SO_4^{2-}}^{org}}{m_{SO_4^{2-}}^{aq}\gamma_{SO_4^{2-}}^{aq}}\right) + \ln\left(\frac{m_{UO_2^{2+}}^{org}\gamma_{UO_2^{2+}}^{org}}{m_{UO_2^{2+}}^{aq,0}\gamma_{UO_2^{2+}}^{aq}}\right) + \boldsymbol{i}lnm_{(R_3NH^+)_2}^{org}\gamma_{(R_3NH^+)_2}^{org} + (\boldsymbol{2i}+\boldsymbol{1})(\Phi^{org} - \Phi^{aq})$$

Equation 4

Where m_i is the molality in mol/kg of solvent of the species under equilibrium conditions in either organic phase (superscript org), or aqueous phase (superscript aq), $m_{UO_2^{2+}}^{aq,0}$ is a reference concentration with an activity of 1, $\Phi^{org} - \Phi^{aq}$ is the difference between the osmotic coefficient in the organic phase and in the aqueous phase (approximately equals to 0.2), γ_i represents the activity coefficient of the various species.

The contribution of extracted water is represented here by the deviation of osmotic coefficient from the ideality in the solvents.

The third term denoted "chain term" contains interfacial effects: these are a free energy of micellization, measured via the CAC ($\Delta G_{micellisation}$), as well as a packing frustration term due to the bending of the interface ($\Delta G_{curvature}$).

- *Micellisation term*

The "micellization term" defines the entropic cost of packing monomeric extractant into reverse micelles in the organic phase. To evaluate this term, CAC derived from the SANS measurements are converted into free energy of micellisation thanks to the following equation:

$$\Delta G_{micellisation} = -N_{agg} \ln(CAC)$$

Equation 5

The droplet and the micellization terms are not sufficient to explain the huge gap between the complexation energy and the energy of transfer. Another term related to the aggregation, called the curvature energy has also to be taken into account.

- *Curvature energy*

Curvature energy is associated to the extractant organization around the extracted and co-extracted species.[29,30] It is associated to the variation of shape and size of the reverse aggregates, and is sensitive to standard and effective packing parameter of the extractant when the aggregates are filled orswollen with polar species.

In other words, curvature energy describes the bending energy of the interface between the hydrophilic core of the aggregates and their hydrophobic shell. The hydrophilic cores contain the solubilized water, acid and metallic cations, as well as the polar headgroups of the extractant molecules. The hydrophobic parts of the aggregates consist of the nonpolar alkyl chains of the extractants.

The bending energy of this interface is proportional to the square of the difference between the effective packing parameter of an aggregate p_e, and the spontaneous packing parameter p_s of this one aggregate without any external constraints. The chain term of a reverse micellar aggregate is therefore given by:

$$\Delta G_{curvature} = \frac{\kappa^*}{2} N_{agg} (p_s - p_e)^2$$

Equation 6

Where κ^*, the generalized bending constant, is expressed in k_BT. It describes the energetic contribution per extractant molecule to a certain interface.

Results and discussion

SANS spectra were measured for various tertiary amines diluted deuterated dodecane, after being contacted with aqueous solutions containing 2500 ppm $UO_2(NO_3)_2$ (10.5 mmol/L), 1 mol/L $(NH_4)_2SO_4$ and 0.1 mol/L H_2SO_4 (pH = 1).

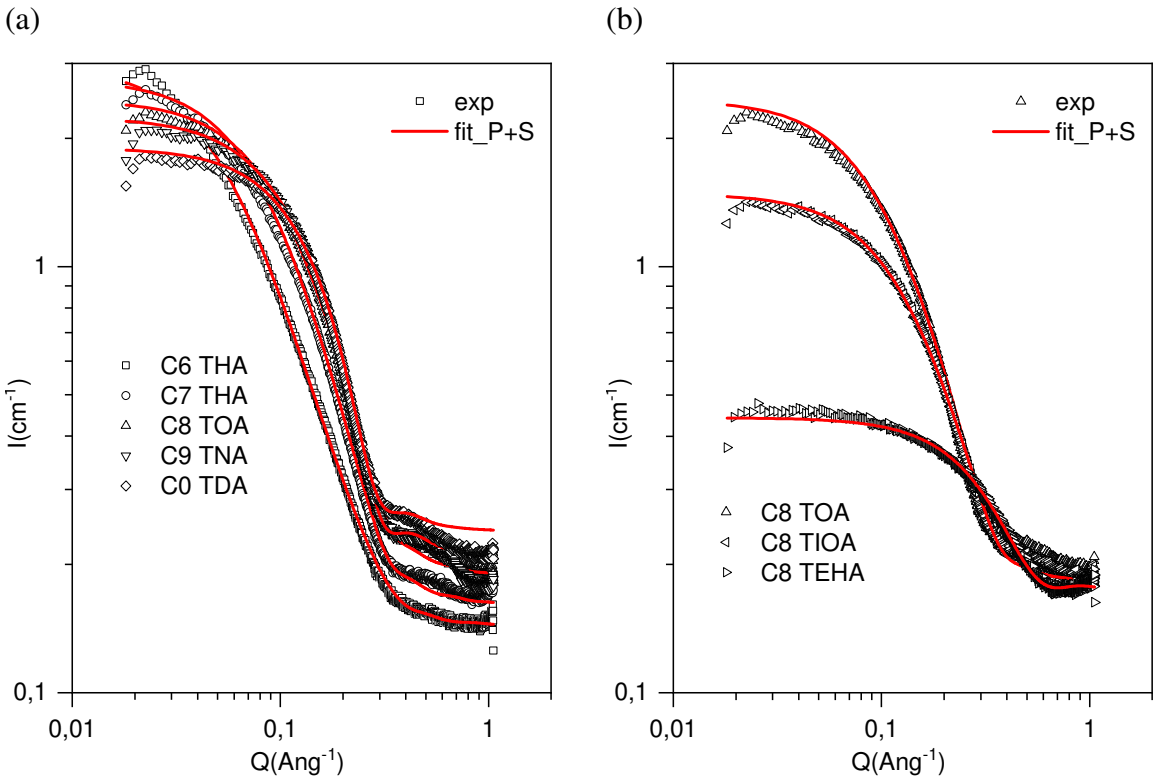

Figure 2. SANS spectra (experiment and fit) of different tertiary amines with linear alkyl chains (a) or with branched alkyl chains (b) (0.2 mol/L) diluted in n-dodecane modified with 5 %vol 1-octanol and contacted with the aqueous phase containing 2500 ppm U(VI), 0.1 mol/L H_2SO_4 and 1 mol/L $(NH_4)_2SO_4$. Each data set is multiplied by 10^n where n runs from 0 to 4 for (a) and from 0 to 2 for (b) starting from the lowermost spectrum.

The absolute scattering spectra and corresponding fitted curves, expressed in cm^{-1}, are plotted as a function of the wave vector Q for the various tertiary amines in Figure 2. It must be noticed that the samples were prepared with deuterated octanol and deuterated dodecane. The contrast being mainly due the hydrogenated/non hydrogenated parts of the samples, scattering signal is then due to the extractant aggregation and does not include the contribution of the octanol molecules that are deuterated and present no contrast with the main solvent. [31]

As mentioned in the first part of this study, the strong increase of intensity at low Q values indicates that tertiary amines form reverse micelle like aggregates. Variations observed

between longer or branched amines suggest moreover that the aggregates have different size distributions or that they present a significant variation of inter-aggregates attraction or both. To complete this interpretation, data were fitted with a model considering a form factor of spherical particles with a core-shell form factor and a Baxter's sticky hard sphere structure factor.

Fitted parameters obtained for tertiary amines with linear and branched alkyl chains are summarized in Table 1 and Table 2.

Table 1. Fitting parameters of SANS spectra of tertiary amines with linear alkyl chains. (Initial organic phases: 0.2 mol/L of tertiary amine diluted in deuterated dodecane modified by 5 %vol. octanol; Initial aqueous phase: 2500 ppm U(VI), 0.1 mol/L H_2SO_4 and 1 mol/L $(NH_4)_2SO_4$.)

N° C	6	7	8	9	10
r_{core} (Å)	6.1±0.2	5.9±0.1	5.8±0.1	5.6±0.2	5.5±0.2
N_{agg}	4.3±0.4	4.2±0.1	4.0±0.2	3.7±0.3	3.4±0.3
$\Delta t_{shell,ND}$ (Å)	4.0±0.1	4.2±0.2	4.2±0.2	4.3±0.1	4.5±0.2
$\Delta t_{shell,D}$ (Å)	2.8±0.1	3.2±0.1	3.4±0.1	3.6±0.2	3.7±0.2
τ^{-1} (k_BT)	10.0±0.5	9.1±0.4	8.3±0.3	7.3±0.3	5.0±0.3

Table 2. Fitting parameters of SANS spectra of tertiary amines with branched alkyl chains.

Branched alkyl chains with 8C	C8 TOA	C8 TIOA	C8 TEHA
r_{core} (Å)	5.8±0.1	5.5±0.1	1.2±0.5
N_{agg}	4.0±0.2	4.2±0.1	0.2±0.3
$\Delta t_{shell,ND}$ (Å)	4.2±0.2	3.9±0.2	6.5±0.2
$\Delta t_{shell,D}$ (Å)	3.4±0.1	3.2±0.1	6.3±0.1
τ^{-1} (k_BT)	8.3±0.3	5.1±0.3	NA

Table 1 shows that the polar core radius r_{core}, decreases with the alkyl chains length of the tertiary amines. As mentioned in part I, it follows the same trend as the concentrations of extracted water and acid, which are assumed to occupy most of the core volume in the core

shell model. The number of extractant per aggregate N_{agg} also follows this trend, but with a slighter variation (from 4.3 to 3.4).

It can also be observed that the thickness of the apolar shell Δt_{shell} increases with increasing alkyl chains length, which is also confirming the core-shell model.

Besides, the stickiness parameter τ^{-1} decreases with the alkyl chain carbon number, which indicates that the aggregates formed by amines with longer chains produce weaker attractive interactions between the aggregates. The evolution of this parameter is consistent with the observation described in paper I: the third phase formation is repelled for extractant having longer alkyl chains. It is also consistent with the evolution of SANS spectra at small angles: scattering intensity decreases, and the plateau appears flatter when the alkyl chains become longer.

It must be noticed here that the stickiness parameters τ^{-1} are high compared to the percolation threshold of ca. $2k_BT$, estimated for such systems. The use of the Baxter model might be discussed as in previous studies,[32–35] but we considered it is sufficiently efficient to estimate the relative trend of attractive interactions when the extractant chains length are modified.

For amines with branched chains, we can notice from Table 2 that TIOA has a slightly smaller polar core than TOA, and a similar Δt_{shell}. In comparison, TEHA which ramification is larger, is only present in the form of monomers and dimers with very small r_{core} and thicker Δt_{shell}. The slightly branched molecule, TIOA forms smaller aggregates than TOA (with r_{core} values 5.5 and 5.8 Å), while no aggregation is observed for TEHA. SANS fitting also allows estimating the stickiness parameter for the branched molecules: τ^{-1} is smaller for TIOA than for TOA, suggesting that the amines with branched alkyl chains form aggregates with less attractive interactions. As the core-shell model reaches its limits for monomeric species, this parameter could not be estimated for TEHA. Comparison between TOA and TIOA confirms however quantitatively the observation commonly noticed in literature that branched alkyl chains quenches the formation of the third phase.

Thermodynamic balance

As described in the previous section, the thermodynamic balance is established according to **Equation 1**, which consists in expressing the transfer energy of uranium as a function of the complexation energy, the droplet term and of the micellisation and curvature free energies. Evaluation of these terms is described in the following.

- *Uranium Gibbs free energy of transfer*

$\Delta G_{transfer}$ is evaluated per ion from **Equation 2** as a function of the distribution ratio.

Figure 3(a) presents the values of $\Delta G_{transfer}(UO_2^{2+})$ for tertiary amines with different chains length (filled circles) and branching (open circles). The transfer energy of uranium per aggregate $\Delta G_{transfer}(UO_2^{2+})$ exhibits a quasi-constant shape with alkyl chain carbon number, which is consistent with the trend observed for D_U.

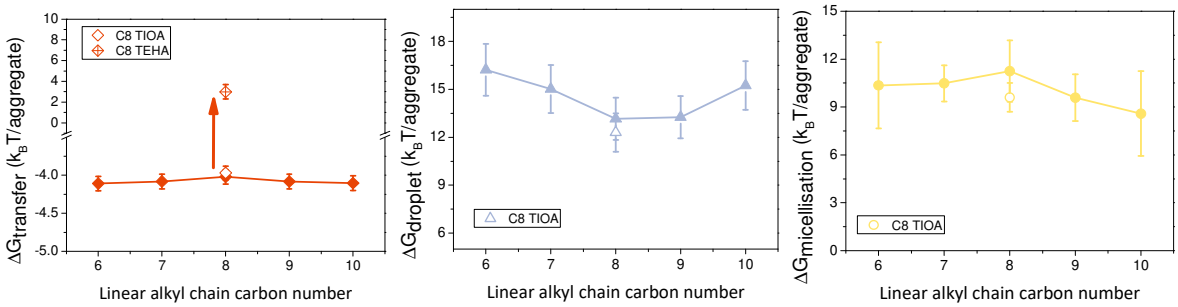

Figure 3. (a) Uranium free energy of transfer; (b) Droplet free Gibbs energy related to the confinement of the electrolyte in the polar core of reverse micelles plotted as a function of alkyl chains length of tertiary amines; (c) Free energy related to the entropy of monomeric extractant in the organic phase which hinders micellization. The values of tertiary amines with C8-based branched chains are also plotted in the same figures.

$\Delta G_{transfer}$ of TOA and TIOA are found to be close to -4 k_BT/agg. TEHA has a positive $\Delta G_{transfer}$ value as it does not extract any uranyl.

Inhibitors due to aggregation

- *Droplet term*

The droplet term is calculated from **Equation 4**, for which the stoichiometric coefficient ***i*** and ***j*** of H_2SO_4 and H_2O in the aggregates containing **1** uranyl must be evaluated. For this, it was considered that the aggregates with and without uranyl have the same volume and aggregation number N_{agg}. Considering the molecular volumes of UO_2SO_4, H_2SO_4 and H_2O (185 Å^3, 89 Å^3 and 30 Å^3 respectively), it was therefore estimated that the volume occupied by one uranyl in the aggregates containing one uranyl ($agg_{with\ UO_2^{2+}}$) is replaced by 3 water and 1 acid molecules in the aggregates with no uranyl ($agg_{no\ UO_2^{2+}}$). The stoichiometry of the polar species in the aggregates was therefore taken as follows: In $agg_{with\ UO_2^{2+}}$, there are **1** UO_2SO_4, ***i*** H_2SO_4 and ***j*** H_2O; while in $agg_{no\ UO_2^{2+}}$, there are **0** UO_2SO_4, **(*i* + 1)** H_2SO_4 and **(*j* + 3)** H_2O.

The stoichiometric coefficients **i** and **j** in aggregates with uranyl were calculated from the average stoichiometric coefficient of UO_2SO_4, H_2SO_4 and H_2O in all the aggregates (noted $N_{UO_2^{2+}}$, $N_{H_2SO_4}$ and N_{H_2O}). Assuming α the proportion of the aggregates being $agg_{with\ UO_2^{2+}}$, and 1- α the proportion of $agg_{no\ UO_2^{2+}}$, we have:

$$N_{UO_2^{2+}} = \alpha \times 1 + (1-\alpha) \times 0$$

$$N_{H_2SO_4} = \alpha \times \boldsymbol{i} + (1-\alpha) \times (\boldsymbol{i}+\mathbf{1})$$

$$N_{H_2O} = \alpha \times \boldsymbol{j} + (1-\alpha) \times (\boldsymbol{j}+\mathbf{3})$$

Equation 7

Where $N_{UO_2^{2+}}$, $N_{H_2SO_4}$ and N_{H_2O} can be calculated from the experimental data with the following equation:

$$N_{UO_2^{2+}}, N_{H_2SO_4}\ N_{H_2O} = \frac{N_{agg}}{[extractant] - CAC} \times [species]_{org}$$

Equation 8

The molalities and stoichiometric coefficients results are presented in Supporting Information in Table S3 and S4.

Another parameter to determine to evaluate the droplet term from **Equation 4** is the activity coefficient of the tertiary amines, $\gamma^{org}_{(R_3NH^+)_2}$. It is a difficult parameter to evaluate as activity coefficient are rarely available for organic species.[36,37] We could however find that $\gamma^{org}_{(R_3NH^+)_2}/(\gamma^{org}_{R_3N})^2$ remains constant for wide concentration range of amine and acid.[38] For sake of simplicity, we considered that all the amines are fully protonated and that $\gamma^{org}_{(R_3NH^+)_2}$ equals to 1.

Equation 4 becomes therefore:

$$\Delta G_{bulk}(UO_2^{2+}) = \boldsymbol{i} \ln\left(\frac{m^{org}_{SO_4^{2-}}\gamma^{org}_{SO_4^{2-}}}{m^{aq}_{SO_4^{2-}}\gamma^{aq}_{SO_4^{2-}}}\right) + \ln\left(\frac{m^{org}_{UO_2^{2+}}\gamma^{org}_{UO_2^{2+}}}{m^{aq,0}_{UO_2^{2+}}\gamma^{aq}_{UO_2^{2+}}}\right) + \boldsymbol{i} ln m^{org}_{(R_3NH^+)_2} + (\mathbf{2}\boldsymbol{i}+\mathbf{1})(\Phi^{org} - \Phi^{aq})$$

Equation 9

Based on these results, the droplet term was estimated and plotted in Figure 3(b).

Results show that the droplet term acts as a strong inhibitor on the transfer energy of uranyl. A slight decrease of the droplet term free energy is observed for higher alkyl chains length, varying from 16 to 13 k_BT/agg, which is consistent with less entropic cost when less polar species are confined in the polar cores. A slight minimization is also observed at C8 TOA.

For branched molecules, $\Delta G_{droplet}$ is slightly decreased. $\Delta G_{droplet}$ of C8 TIOA is 12.3 k_BT/agg, while for C8 TEHA, the value is close to zero, since the polar core of this amine is too small to solubilize any polar species inside.

- *Micellisation term*

The micellization term is calculated from **Equation 5** thanks to the CAC determination presented in the first part of this paper. Results are plotted in Figure 3(c). Due to the entropy cost to form aggregates with the monomeric extractants, it is another predominant inhibitor of extraction. Results show that C8 TOA has a slightly larger micellization free energy (11.2 k_BT/agg) while the values of the other linear amines show a gradual and slight decrease from 10.3 to 8.6 k_BT/agg.

C8 TIOA, the amine with relatively small branched groups, shows a smaller micellization free energy of 9.6 k_BT/agg than C8 TOA. $\Delta G_{micellisation}$ of C8 TEHA is negligeable since it does not form micelles in dodecane.

- *Curvature & Complexation energy*

Gathering all the information, two remaining parameters need to be estimated: the complexation energy and the curvature energy which depends both on effective and standard packing parameter and on the bending constant κ^* (**Equation 6**). Order of magnitude of these parameters are accessible in literature,[39–43] but they have never been estimated for tertiary amines systems.

As the chelation site of the tertiary amines remains constant, we considered here a constant complexation energy of -35 k_B T/ion, which is consistent with the values estimated for similar systems.[19,20]

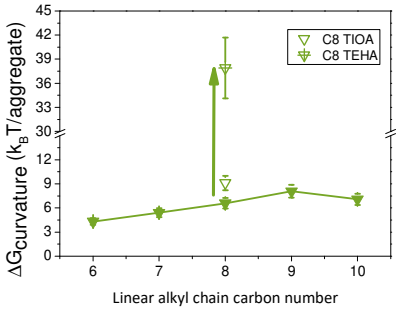

Figure 4. Considering a constant $\Delta G_{complexation}$ the chain free energy ΔG_{chain} is plotted as a function of alkyl chains length. The values of tertiary amines with branched chains are also compared in the same figures.

With this asumption an estimation of the curvature free energy was deduced and is plotted in Figure 4. It shows an increase from 4.3 to 8.1 k_BT/aggregate when the alkyl chain length is increased, and from 6.6 to 9.1 k_BT/agg from TOA to the slightly branched TIOA. For the bulkier branching (TEHA), a significant increase of $\Delta G_{curvature}$ reaching 37.9 k_BT/agg is estimated. This result shows that for TEHA, the curvature energy almost counter balanced by itself the complexation free energy.

Sum of all contributions

To better illustrate the influence of each contribution on the transfer energy, a sum of the main driving forces is plotted in Figure 5.

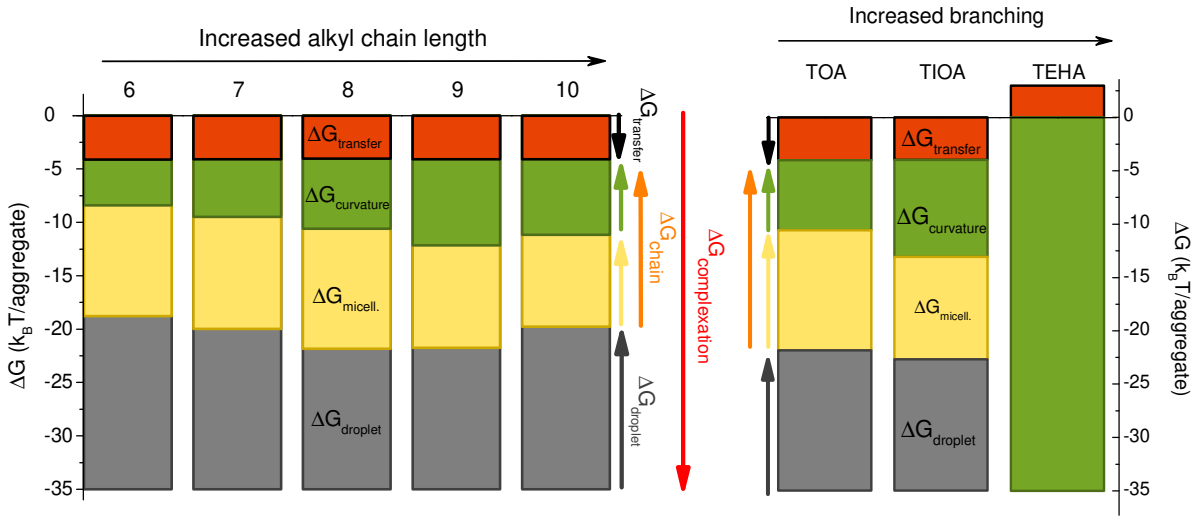

Figure 5. The main contributions are summed to illustrate their influence on the uranium transfer energy of tertiary amines and plotted as a function of alkyl chains length a) and branching b).

Effect of alkyl chains length:

- The droplet term $\Delta G_{droplet}$ and the micellization energy $\Delta G_{micellisation}$ are responsible for respectively 40 % and 20 % of the complexation energy loss. They appear almost constant over the whole range of alkyl chains length.
- Curvature energy is secondary inhibitors of the complexation, which is more sensitive to the alkyl chain configuration. The tertiary amine with the shortest alkyl chains (C6 THA) present the lowest curvature energy. The higher curvature energy obtained for the longer alkyl chains is associated to lower water and acid extraction. Long chain configurations being less favorable, the aggregates can hardly swell and extract polar species.

- The resulting transfer energy $\Delta G_{transfer}$ is quasi-constant, with a value of approximately -4 k_BT/ion. After counter balancing all the inhibitor terms, it appears that only 11 % of the complexation energy is necessary to induce the transfer of uranyl from aqueous phase to organic phase, which is in agreement with the study previously published on DMDOHEMA and HDEHP systems.[20,24]

Effect of chains branching:

When the branched groups become larger and closer to the polar head (from TOA to TIOA and TEHA), the inhibitors ΔG_{bulk} and $\Delta G_{micellisation}$ become less important. In opposition, the significance of ΔG_{chain} increases and becomes large enough to counterbalance $\Delta G_{complexation}$. Consequently, the extraction efficiency of the TEHA amine vanishes to zero.

Overall, this thermodynamic approach shows that the driving forces based on the tertiary amines aggregation are significantly responsible for the extraction efficiency of water and acid. In return, uranium extraction is mainly controlled by the amine's complexation. The free energy of transfer depends only weakly on the linear alkyl chain lengths: variations of curvature term is compensated by variation of the cost of micellisation.

For different alkyl chain branching the situation is different. For moderate branching located far from the chelation site, effect is small and comparable to the entropy of configuration of branched chains.[44,45] However, for stronger branching located closer to the chelation site, the spontaneous curvature of the aggregates is much lower than the polar core and the frustration energy of bending increases so much that free energy of extraction changes sign.

Conclusion

SANS analysis confirmed that longer or branched alkyl chains markedly affects the supramolecular self-assembly of the tertiary amines into smaller reverse micelle like aggregates. It primarily induces a decrease of the water and acid extracted, and secondarily induces a decrease of uranium extraction. SANS fitting also shows that longer of branched alkyl chains leads to less third phase formation thanks to reduced attractive interactions between the aggregates.

The "ienaic" approach was further applied to establish a thermodynamic balance of the driving and inhibiting forces responsible for the transfer of uranium by the various tertiary amines. Considering both the complexation and aggregation abilities of the extractants, this

approach showed that the two most important inhibitors of the uranium transfer are the droplet and micellization free energies, which are due to the extractant aggregation. Assuming a constant complexation energy, the chain free energy was shown to be a secondary inhibitor to uranium transfer and to increase slightly with the alkyl chains length.

The global thermodynamic balance indicates moreover that uranium extraction remains globally constant for the various alkyl chain lengths because it is mostly controlled by the complexation ability of the extractant molecules and poorly affected by extractant aggregation. In comparison, extraction of water and acid is strongly influenced by the aggregation of tertiary amines and significantly reduced when longer alkyl chains are employed, because of a larger curvature energy.

The situation is slightly different for bulky branched alkyl chains which significantly influence the transfer energy of uranium. When the branched group of alkyl chains is large and close to the polar head, the chain free energy becomes such an important inhibitor that no complexation nor aggregation can be achieved. This huge constraint almost counterbalances the complexation free energy and results in a huge drop of extraction efficiency towards water, acid and uranium. If branching induces high enough spontaneous packing (typically above 4), the aggregation cannot take place for steric reasons (frustration energy too high) and the extraction is completely quenched.

This combined colloidal approach and "ienaic" thermodynamic analysis does not only allow understanding the effects of alkyl chains configuration on uranium extraction, but it also provides promising direction to optimize selective uranium extraction towards competitors as Zr, Th, and Pu etc. It has been reported that, tuning the elongation of alkyl chains or introducing branching groups can optimize the selective extraction of U/Th by trialkyl phosphates,[46,47] or increase the selectivity U/Zr of carbamide extractants.[48,49] However, these properties have never been studied with a colloidal approach and related to aggregation mechanisms. Since the polar cores volume is strongly influenced by the alkyl chain's structure, extraction of competing elements by solubilization can be monitored by tuning the alkyl chain configuration. This effect could be exploited to control the selectivity, and in the peculiar case of uranium with tertiary amines, it could also provide new options to improve the degradation problem of tertiary amines encountered in the AMEX process, as a higher selectivity toward vanadium is expected to reduce amines degradation problems.

Acknowledgements

This research was supported financially by NEEDS program and CEA. We deeply thank ILL for the beamtime allocation on D16 (https://doi.ill.fr/10.5291/ILL-DATA.9-10-1637).

References

[1] J. Rydberg, Solvent Extraction Principles and Practice, Revised and Expanded, 2004. https://doi.org/10.1201/9780203021460.

[2] D. Bourgeois, A. El Maangar, S. Dourdain, Importance of weak interactions in the formulation of organic phases for efficient liquid/liquid extraction of metals, Curr. Opin. Colloid Interface Sci. 46 (2020) 36–51. https://doi.org/10.1016/j.cocis.2020.03.004.

[3] T. Zemb, C. Bauer, P. Bauduin, L. Belloni, C. Déjugnat, O. Diat, V. Dubois, J.F. Dufrêche, S. Dourdain, M. Duvail, C. Larpent, F. Testard, S. Pellet-Rostaing, Recycling metals by controlled transfer of ionic species between complex fluids: en route to "ienaics," Colloid Polym. Sci. 293 (2014). https://doi.org/10.1007/s00396-014-3447-x.

[4] E.A. Mowafy, H.F. Aly, Extraction behaviors of trivalent lanthanides from nitrate medium by selected substituted malonamides, Solvent Extr. Ion Exch. 24 (2006) 677–692. https://doi.org/10.1080/07366290600762322.

[5] B. Gannaz, R. Chiarizia, M.R. Antonio, C. Hill, G. Cote, Extraction of lanthanides (III) and Am (III) by mixtures of malonamide and dialkkyphosphoric acid, Solvent Extr. Ion Exch. 25 (2007) 313–337. https://doi.org/10.1080/07366290701285512.

[6] Q. Tian, M.A. Hughes, The mechanism of extraction of HNO3 and neodymium with diamides, Hydrometallurgy. 36 (1994) 315–330. https://doi.org/10.1016/0304-386X(94)90029-9.

[7] C. Tanford, The Hydrophobic Effect: Formation of Micelles and Biological Membranes (2nd Edition), 1980.

[8] L. Berthon, L. Martinet, F. Testard, C. Madic, T. Zemb, Solvent penetration and sterical stabilization of reverse aggregates based on the DIAMEX process extracting molecules: Consequences for the third phase formation, Solvent Extr. Ion Exch. 25 (2007) 545–576. https://doi.org/10.1080/07366290701512576.

[9] M.C. Dul, B. Braibant, S. Dourdain, S. Pellet-Rostaing, D. Bourgeois, D. Meyer, Perfluoroalkyl- vs alkyl substituted malonamides: Supramolecular effects and consequences for extraction of metals, J. Fluor. Chem. 200 (2017) 59–65. https://doi.org/10.1016/j.jfluchem.2017.06.001.

[10] J. Rey, S. Dourdain, L. Berthon, J. Jestin, S. Pellet-Rostaing, T. Zemb, Synergy in Extraction System Chemistry: Combining Configurational Entropy, Film Bending, and

Perturbation of Complexation, Langmuir. 31 (2015) 7006–7015. https://doi.org/10.1021/acs.langmuir.5b01478.

[11] C. Déjugnat, L. Berthon, V. Dubois, Y. Meridiano, S. Dourdain, D. Guillaumont, S. Pellet-Rostaing, T. Zemb, Liquid-Liquid Extraction of Acids and Water by a Malonamide: I-Anion Specific Effects on the Polar Core Microstructure of the Aggregated Malonamide, Solvent Extr. Ion Exch. 32 (2014) 601–619. https://doi.org/10.1080/07366299.2014.940229.

[12] C. Erlinger, D. Gazeau, T. Zemb, C. Madic, L. Lefrançois, M. Hebrant, C. Tondre, Effect of nitric acid extraction on phase behavior, microstructure and interactions between primary aggregates in the system dimethyldibutyltetradecylmalonamide (DMDBTDMA) / n-dodecane / water: A phase analysis and small angle X-ray scattering (SAXS) char, Solvent Extr. Ion Exch. 16 (1998) 707–738. https://doi.org/10.1080/07366299808934549.

[13] C. Déjugnat, S. Dourdain, V. Dubois, L. Berthon, S. Pellet-Rostaing, J.F. Dufrêche, T. Zemb, Reverse aggregate nucleation induced by acids in liquid-liquid extraction processes, Phys. Chem. Chem. Phys. 16 (2014) 7339–7349. https://doi.org/10.1039/c4cp00073k.

[14] R.J. Ellis, T.L. Anderson, M.R. Antonio, A. Braatz, M. Nilsson, A SAXS study of aggregation in the synergistic TBP-HDBP solvent extraction system, J. Phys. Chem. B. 117 (2013) 5916–5924. https://doi.org/10.1021/jp401025e.

[15] Y. Liu, M. Lee, G. Senanayake, Potential connections between the interaction and extraction performance of mixed extractant systems: A short review, J. Mol. Liq. 268 (2018) 667–676. https://doi.org/10.1016/j.molliq.2018.07.097.

[16] O. Pecheur, S. Dourdain, D. Guillaumont, J. Rey, P. Guilbaud, L. Berthon, M.C. Charbonnel, S. Pellet-Rostaing, F. Testard, Synergism in a HDEHP/TOPO Liquid-Liquid Extraction System: An Intrinsic Ligands Property?, J. Phys. Chem. B. 120 (2016) 2814–2823. https://doi.org/10.1021/acs.jpcb.5b11693.

[17] M. Špadina, K. Bohinc, T. Zemb, J.F. Dufrêche, Colloidal Model for the Prediction of the Extraction of Rare Earths Assisted by the Acidic Extractant, Langmuir. 35 (2019) 3215–3230. https://doi.org/10.1021/acs.langmuir.8b03846.

[18] D. Stamberga, M.R. Healy, V.S. Bryantsev, C. Albisser, Y. Karslyan, B. Reinhart, A. Paulenova, M. Foster, I. Popovs, K. Lyon, B.A. Moyer, S. Jansone-Popova, Structure Activity Relationship Approach toward the Improved Separation of Rare-Earth

Elements Using Diglycolamides, Inorg. Chem. 59 (2020) 17620–17630. https://doi.org/10.1021/acs.inorgchem.0c02861.

[19] T. Zemb, M. Duvail, J.F. Dufrêche, Reverse aggregates as adaptive self-assembled systems for selective liquid-liquid cation extraction, Isr. J. Chem. 53 (2013) 108–112. https://doi.org/10.1002/ijch.201200091.

[20] J.F. Dufrêche, T. Zemb, Effect of long-range interactions on ion equilibria in liquid-liquid extraction, Chem. Phys. Lett. 622 (2015) 45–49. https://doi.org/10.1016/j.cplett.2014.11.028.

[21] M. Špadina, J.F. Dufrêche, S. Pellet-Rostaing, S. Marčelja, T. Zemb, Molecular Forces in Liquid-Liquid Extraction, Langmuir. (2021). https://doi.org/10.1021/acs.langmuir.1c00673.

[22] M. Špadina, K. Bohinc, T. Zemb, J.F. Dufrêche, Multicomponent Model for the Prediction of Nuclear Waste/Rare-Earth Extraction Processes, Langmuir. 34 (2018) 10434–10447. https://doi.org/10.1021/acs.langmuir.8b01759.

[23] M. Špadina, K. Bohinc, T. Zemb, J.F. Dufrêche, Synergistic Solvent Extraction Is Driven by Entropy, ACS Nano. 13 (2019) 13745–13758. https://doi.org/10.1021/acsnano.9b07605.

[24] J. Rey, M. Bley, J.F. Dufrêche, S. Gourdin, S. Pellet-Rostaing, T. Zemb, S. Dourdain, Thermodynamic Description of Synergy in Solvent Extraction: II Thermodynamic Balance of Driving Forces Implied in Synergistic Extraction, Langmuir. 33 (2017) 13168–13179. https://doi.org/10.1021/acs.langmuir.7b02068.

[25] C. Erlinger, L. Belloni, T. Zemb, C. Madic, Attractive interactions between reverse aggregates and phase separation in concentrated malonamide extractant solutions, Langmuir. 15 (1999) 2290–2300. https://doi.org/10.1021/la980313w.

[26] B.W. Ninham, I.S. Barnes, S.T. Hyde, P.J. Derian, T.N. Zemb, Random connected cylinders: A new structure in three-component microemulsions, EPL. 4 (1987) 561–568. https://doi.org/10.1209/0295-5075/4/5/009.

[27] P. Debye, H.R. Anderson, H. Brumberger, Scattering by an inhomogeneous solid. II. the correlation function and its application, J. Appl. Phys. 28 (1957) 679–683. https://doi.org/10.1063/1.1722830.

[28] L. Ornstein, F. Zernike, Accidental deviations of density and opalescence at the critical point of a single substance, Proc. Akad. Sci.(Amsterdam). XVII (1914) 793–806. https://ci.nii.ac.jp/naid/20000793087 (accessed December 17, 2021).

[29] Y. Chen, M. Duvail, P. Guilbaud, J.F. Dufrêche, Stability of reverse micelles in rare-earth separation: A chemical model based on a molecular approach, Phys. Chem. Chem. Phys. 19 (2017) 7094–7100. https://doi.org/10.1039/c6cp07843e.

[30] D.M. Brigham, A.S. Ivanov, B.A. Moyer, L.H. Delmau, V.S. Bryantsev, R.J. Ellis, Trefoil-Shaped Outer-Sphere Ion Clusters Mediate Lanthanide(III) Ion Transport with Diglycolamide Ligands, J. Am. Chem. Soc. 139 (2017) 17350–17358. https://doi.org/10.1021/jacs.7b07318.

[31] Z. Lu, S. Dourdain, S. Pellet-Rostaing, Understanding the Effect of the Phase Modifier n-Octanol on Extraction, Aggregation, and Third-Phase Appearance in Solvent Extraction, Langmuir. 36 (2020) 12121–12129. https://doi.org/10.1021/acs.langmuir.0c01554.

[32] A.G. Baldwin, M.J. Servis, Y. Yang, N.J. Bridges, D.T. Wu, J.C. Shafer, The structure of tributyl phosphate solutions: Nitric acid, uranium (VI), and zirconium (IV), J. Mol. Liq. 246 (2017) 225–235. https://doi.org/10.1016/j.molliq.2017.09.032.

[33] R. Motokawa, T. Kobayashi, H. Endo, J. Mu, C.D. Williams, A.J. Masters, M.R. Antonio, W.T. Heller, M. Nagao, A Telescoping View of Solute Architectures in a Complex Fluid System, ACS Cent. Sci. 5 (2019) 85–96. https://doi.org/10.1021/acscentsci.8b00669.

[34] J. Mu, R. Motokawa, K. Akutsu, S. Nishitsuji, A.J. Masters, A Novel Microemulsion Phase Transition: Toward the Elucidation of Third-Phase Formation in Spent Nuclear Fuel Reprocessing, J. Phys. Chem. B. 122 (2018) 1439–1452. https://doi.org/10.1021/acs.jpcb.7b08515.

[35] R. Motokawa, S. Suzuki, H. Ogawa, M.R. Antonio, T. Yaita, Microscopic structures of tri-n-butyl phosphate/n-octane mixtures by X-ray and neutron scattering in a wide q range, J. Phys. Chem. B. 116 (2012) 1319–1327. https://doi.org/10.1021/jp210808r.

[36] A.S. Kertes, G. Markovits, Activity coefficients, aggregation, and thermodynamics of tridodecylammonium salts in nonpolar solvents, J. Phys. Chem. 72 (1968) 4202–4210. https://doi.org/10.1021/j100858a045.

[37] J.I. Bullock, S.S. Choi, D.A. Goodrick, D.G. Tuck, E.J. Woodhouse, Organic phase species in the extraction of mineral acids by methyldioctylamine in chloroform, J. Phys. Chem. 68 (1964) 2687–2696. https://doi.org/10.1021/j100791a052.

[38] V. Shmidt, Amine Extraction, Israel Program for Scientific Translations, 1971.

[39] A. Fogden, S.T. Hyde, G. Lundberg, Bending energy of surfactant films, J. Chem. Soc. Faraday Trans. 87 (1991) 949–955. https://doi.org/10.1039/FT9918700949.

[40] F. Testard, T. Zemb, Excess of solubilization and curvature in nonionic microemulsions, J. Colloid Interface Sci. 219 (1999) 11–19. https://doi.org/10.1006/jcis.1999.6466.

[41] O. Holderer, H. Frielinghaus, M. Monkenbusch, M. Klostermann, T. Sottmann, D. Richter, Experimental determination of bending rigidity and saddle splay modulus in bicontinuous microemulsions, Soft Matter. 9 (2013) 2308–2313. https://doi.org/10.1039/c2sm27449c.

[42] T. Hellweg, D. Langevin, Bending elasticity of the surfactant monolayer in droplet microemulsions: Determination by a combination of dynamic light scattering and neutron spin-echo spectroscopy, Phys. Rev. E - Stat. Physics, Plasmas, Fluids, Relat. Interdiscip. Top. 57 (1998) 6825–6834. https://doi.org/10.1103/PhysRevE.57.6825.

[43] B. Farago, D. Richter, J.S. Huang, S.A. Safran, S.T. Milner, Shape and size fluctuations of microemulsion droplets: The role of cosurfactant, Phys. Rev. Lett. 65 (1990) 3348–3351. https://doi.org/10.1103/PhysRevLett.65.3348.

[44] A. Czajka, G. Hazell, J. Eastoe, Surfactants at the Design Limit, Langmuir. 31 (2015) 8205–8217. https://doi.org/10.1021/acs.langmuir.5b00336.

[45] M. Sagisaka, T. Narumi, M. Niwase, S. Narita, A. Ohata, C. James, A. Yoshizawa, E. Taffin De Givenchy, F. Guittard, S. Alexander, J. Eastoe, Hyperbranched hydrocarbon surfactants give fluorocarbon-like low surface energies, Langmuir. 30 (2014) 6057–6063. https://doi.org/10.1021/la501328s.

[46] K.B. Rakesh, A. Suresh, P.R. Vasudeva Rao, Studies on Third Phase Formation in the Extraction of Th(NO3)4 by Tri-iso-amyl Phosphate in n-alkane Diluents, Sep. Sci. Technol. 48 (2013) 2761–2770. https://doi.org/10.1080/01496395.2013.816322.

[47] A. Suresh, T.G. Srinivasan, P.R. Vasudeva Rao, The effect of the structure of trialkyl phosphates on their physicochemical properties and extraction behavior, Solvent Extr. Ion Exch. 27 (2009) 258–294. https://doi.org/10.1080/07366290802674481.

[48] C. Berger, C. Marie, D. Guillaumont, E. Zekri, L. Berthon, Extraction of Uranium(VI) and Plutonium(IV) with Tetra-Alkylcarbamides, Solvent Extr. Ion Exch. 37 (2019) 111–125. https://doi.org/10.1080/07366299.2019.1630095.

[49] A. Artese, S. Dourdain, N. Boubals, T. Dumas, P.L. Solari, D. Menut, L. Berthon, P. Guilbaud, S. Pellet-Rostaing, Evidence of Supramolecular Origin of Selectivity in Solvent Extraction of Bifunctional Amidophosphonate Extractants with Different Configurations, Solvent Extr. Ion Exch. (2021). https://doi.org/10.1080/07366299.2021.1961433.